

See discussions, stats, and author profiles for this publication at: <https://www.researchgate.net/publication/23302022>

# Hybridization of Pulsed-Q Dissociation and Collision-Activated Dissociation in Linear Ion Trap Mass Spectrometer for iTRAQ Quantitation

ARTICLE *in* JOURNAL OF PROTEOME RESEARCH · NOVEMBER 2008

Impact Factor: 4.25 · DOI: 10.1021/pr800403z · Source: PubMed

---

CITATIONS

49

---

READS

73

6 AUTHORS, INCLUDING:



[Huoming Zhang](#)

King Abdullah University of Science and Te...

46 PUBLICATIONS 902 CITATIONS

SEE PROFILE

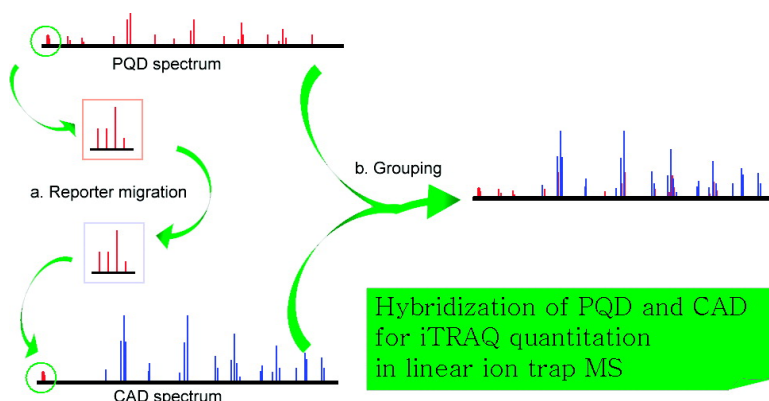
Article

## Hybridization of Pulsed-Q Dissociation and Collision-Activated Dissociation in Linear Ion Trap Mass Spectrometer for iTRAQ Quantitation

Tiannan Guo, Chee Sian Gan, Huoming Zhang, Yi Zhu, Oi Lian Kon, and Siu Kwan Sze

*J. Proteome Res.*, **2008**, 7 (11), 4831-4840 • DOI: 10.1021/pr800403z • Publication Date (Web): 07 October 2008

Downloaded from <http://pubs.acs.org> on November 19, 2008



### More About This Article

Additional resources and features associated with this article are available within the HTML version:

- Supporting Information
- Access to high resolution figures
- Links to articles and content related to this article
- Copyright permission to reproduce figures and/or text from this article

[View the Full Text HTML](#)



**ACS Publications**  
High quality. High impact.

Journal of Proteome Research is published by the American Chemical Society.  
1155 Sixteenth Street N.W., Washington, DC 20036

## Hybridization of Pulsed-Q Dissociation and Collision-Activated Dissociation in Linear Ion Trap Mass Spectrometer for iTRAQ Quantitation

Tiannan Guo,<sup>†,‡</sup> Chee Sian Gan,<sup>†</sup> Huoming Zhang,<sup>†</sup> Yi Zhu,<sup>†</sup> Oi Lian Kon,<sup>‡</sup> and Siu Kwan Sze<sup>\*,†</sup>

*School of Biological Sciences, Nanyang Technological University, 60 Nanyang Drive, Singapore 637551, and  
Division of Medical Sciences, National Cancer Centre Singapore, 11 Hospital Drive, Singapore 169610*

Received June 3, 2008

Coupling of multiplex isobaric tags for relative and absolute quantitation (iTRAQ) to a sensitive linear ion trap (LTQ) mass spectrometer (MS) is a challenging, but highly promising approach for quantitative high-throughput proteomic profiling. Integration of the advantages of pulsed-Q dissociation (PQD) and collision-activated dissociation (CAD) fragmentation methods into a PQD–CAD hybrid mode, together with PQD optimization and data manipulation with a bioinformatics algorithm, resulted in a robust, sensitive and accurate iTRAQ quantitative proteomic workflow. The workflow was superior to the default PQD setting when profiling the proteome of a gastric cancer cell line, SNU5. Taken together, we established an optimized PQD-CAD hybrid workflow in LTQ-MS for iTRAQ quantitative proteomic profiling that may have wide applications in biological and biomedical research.

**Keywords:** quantitative proteomics • iTRAQ • pulsed-Q dissociation • collision-activated dissociation • ion trap • gastric cancer

### Introduction

Simultaneous quantitative proteomic profiling of multiple biological states in a high-throughput manner holds significant potential for biological and biomedical discovery. This has encouraged rapid development in biological mass spectrometry (MS) methods for quantitative proteomics.<sup>1–4</sup> As MS is not inherently quantitative, protein or peptide samples are usually labeled with stable isotopes for relative quantitation. Quantitative information can be acquired either from MS spectra, such as stable isotope labeling by amino acids in cell culture (SILAC),<sup>5</sup> or MS/MS spectra, like isobaric tags for relative and absolute quantitation (iTRAQ).<sup>6</sup>

iTRAQ is currently the most widely used approach for high-throughput protein quantitation at the MS/MS level. It enables simultaneous quantitation of up to 4 (4-plex iTRAQ) or 8 (8-plex iTRAQ) different biological samples. Furthermore, iTRAQ stable isotope reagents are incorporated “post-harvest” to protein samples at peptide level via chemical approaches,<sup>1,6</sup> allowing accurate protein quantitation from diverse origins, including cell lines, tissue samples, biological fluids, and so forth. Linear ion trap MS is one of the most extensively employed MS instruments in current proteomic research, mainly due to its unsurpassed sensitivity, as well as high ion capacity, fast scan rate, ease of use, and relatively low cost.<sup>7,8</sup> Application of iTRAQ in linear ion trap mass spectrometers has been a great challenge because most of the low  $m/z$  iTRAQ

reporter ions are not detected/captured in the ion trap after CAD fragmentation.<sup>9</sup> iTRAQ reporter ions can be detected in many mass spectrometers in MS/MS mode, such as MALDI-TOF-TOF and Q-TOF,<sup>6</sup> with the exception of the ion trap. In theory, iTRAQ reporter ions can only be detected with linear ion trap MS instruments if the precursor ion  $m/z$  is less than 3 times of iTRAQ reporter ions with the CAD fragmentation method.

The recent introduction of a novel fragmentation method, pulsed-Q dissociation (PQD),<sup>10,11</sup> is touted to be a more robust method for iTRAQ reporter ions detection in the linear ion trap MS. PQD fragmentation mode enables low  $m/z$  ions detection through subtle manipulation of the  $Q$ -value during the fragmentation process. In a typical PQD, a high  $Q$ -value, implemented by elevating radio frequency amplitude, is first set to endow kinetic energy to the precursor ions. The subsequent high resonance excitation amplitude, customarily 7 times higher than that in CAD mode, is applied to the precursor ions for a short time. After excitation, the precursor ions are left in the elevated amplitude for a period of time. During this phase, the precursor ions gain enough kinetic energy, begin colliding with helium, thus convert kinetic energy into internal energy, and are finally fragmented. Before significant fragmentation occurs, amplitude is promptly down-regulated to a low level where fragment ions with low  $m/z$ , including iTRAQ reporter ions, are stable in the ion trap.

In the PQD process, three figures of merit, namely, normalized collision energy (CE), activation  $Q$  ( $Q$ ), and activation time ( $T$ ), have substantial influences on the PQD efficiency. Several groups have previously worked on optimizing PQD parameters,<sup>8,11–15</sup> but to date, there is still no uniform consensus for

\* Corresponding author: Dr. Siu Kwan Sze, School of Biological Sciences, Nanyang Technological University, 60 Nanyang Drive, Singapore 637551. E-mail, sksze@ntu.edu.sg; Tel, (+65)6514-1006; fax, (+65)6791-3856.

<sup>†</sup> Nanyang Technological University.

<sup>‡</sup> National Cancer Centre Singapore.

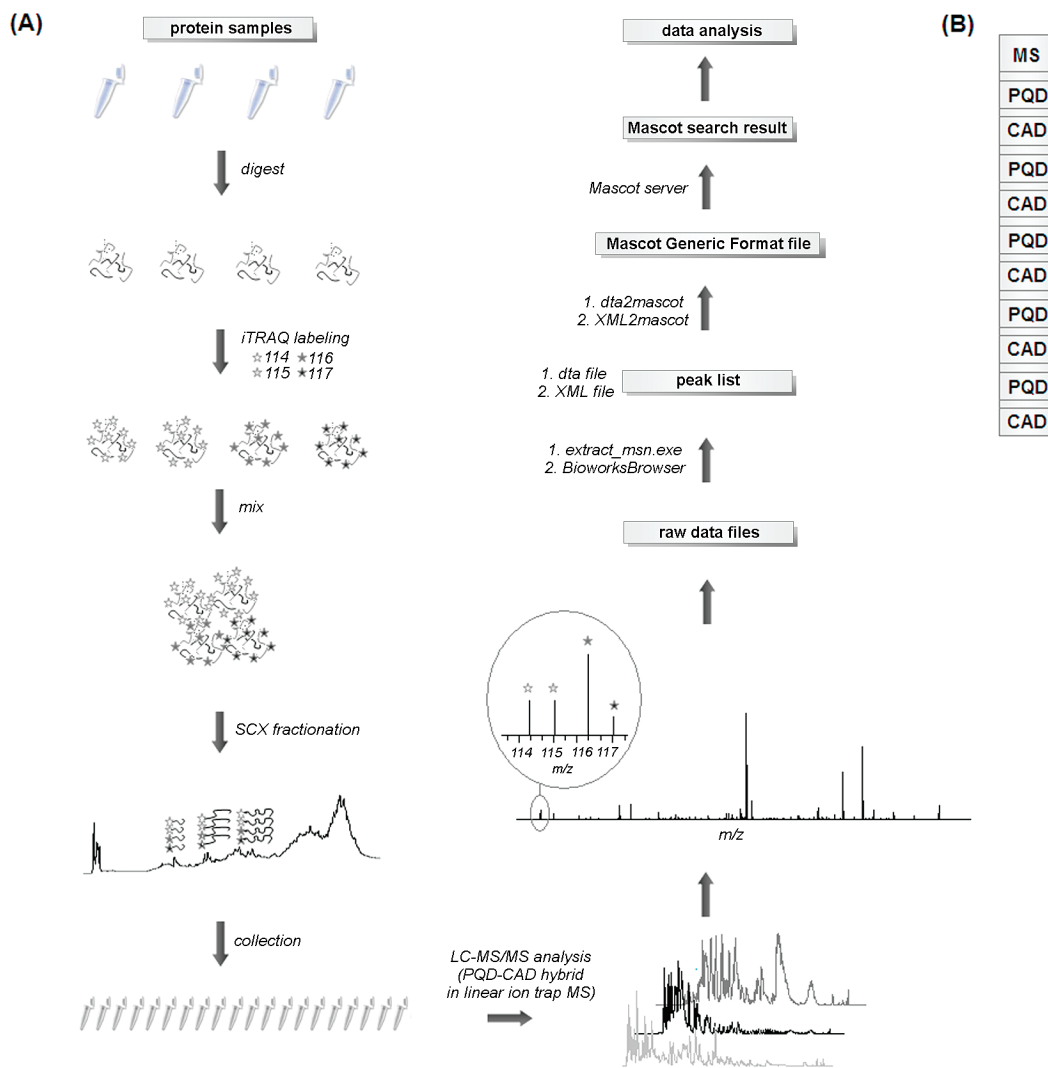


**Figure 1.** Workflow for iTRAQ experiment in linear ion trap mass spectrometer with PQD–CAD hybrid mode. (A) Proteins were digested and labeled with iTRAQ reagents and subsequently mixed. Peptides from cell lysate were fractionated in SCX before they were injected into LC-MS/MS. Peak list files were generated from raw data files using `extract_msn.exe` or `BioworksBrowser` in the format of dta or XML, which can be converted to mascot generic files and submitted to Mascot server for database search. Data were further analyzed in details using in-house perl scripts. (B) In PQD–CAD hybrid mode, each MS scan is followed by 5 (for standard protein mixture) or 10 (for SNU5 cell lysate) pairs of PQD–CAD MS/MS hybrid scans.

an optimized PQD condition. The inadequate PQD efficiency is the bottleneck preventing wide application of linear ion trap MS instruments for iTRAQ quantitation.

Here, we showed experimentally that CAD and PQD both play indispensable and complementary roles for iTRAQ-based quantitation in linear ion trap MS. PQD is relatively inefficient compared with CAD, but unlike CAD, it is able to detect low  $m/z$  fragment ions including iTRAQ reporter ions without limitation of precursor  $m/z$ . In contrast, CAD theoretically detects only iTRAQ reporter ions that are generated from precursors with an  $m/z$  lower than  $114.1 \times 3 \approx 350$  due to the “one-third rule”. Interestingly, CAD generated less iTRAQ reporter numbers, but higher iTRAQ intensities than PQD. On the basis of the results, we combined PQD and CAD into a PQD–CAD hybrid fragmentation mode to integrate the advantages of the two methods. Furthermore, we developed a bioinformatics algorithm and tools for the downstream data analysis. The computational programs written in perl are available upon request for noncommercial applications. To optimize PQD conditions, we altered in stepwise manner three

PQD parameters: CE, Q, and T. Screening of a total of 168 PQD conditions demonstrated an interesting pattern of PQD efficiency upon variation of these parameters. Replicate experiments showed the consistency of the results. The optimal PQD setting was further validated using a gastric cancer cell line, SNU5. Results showed that our optimized setting obtained 300% higher ion intensity, 100% higher iTRAQ reporter ion intensity, 18% more proteins identified and 36% more quantitated peptides than the default setting. Taken together, we established a validated solution for iTRAQ quantitation in linear ion trap MS.

## Materials and Methods

**Protein Sample Preparation.** Standard proteins including chicken ovalbumin, bovine alpha-casein (including subunit 1 and 2), bovine beta-casein, horse cytochrome C, bovine serum albumin, horse myoglobin, and chicken lysozyme were mixed accordingly and dissolved in 0.5 M triethylammonium bicarbonate (TEAB). Gastric cancer cell line SNU5, obtained from ATCC, was cultured at 37 °C in a 5% CO<sub>2</sub>-air atmosphere in

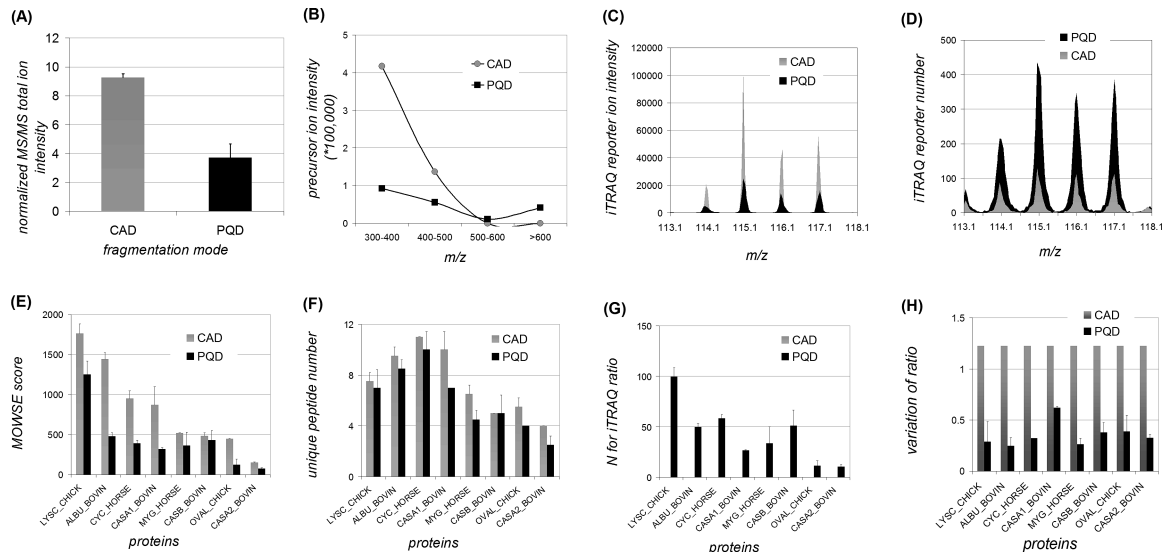


**Figure 2.** Comparison of spectra in PQD and CAD fragmentation modes. The 7-protein mixture (Table 2 in Supporting Information) digests labeled with iTRAQ reagents with the ratio 1:4:2:2 (114:115:116:117) were analyzed in ion trap MS using either PQD (CE = 30%,  $Q = 0.60$ ,  $T = 0.30$  ms) or CAD (CE = 35%,  $Q = 0.25$ ,  $T = 30$  ms) mode with replicates. Normalized MS/MS total ion intensity (A),  $m/z$  distribution of precursors which produce detectable iTRAQ reporter ions (B), iTRAQ reporter total ion intensity (C), iTRAQ reporter total ion number (D), MOWSE score of proteins (E), unique peptide number of proteins (F), N for ratio (G), and variation of ratio (H) were shown.

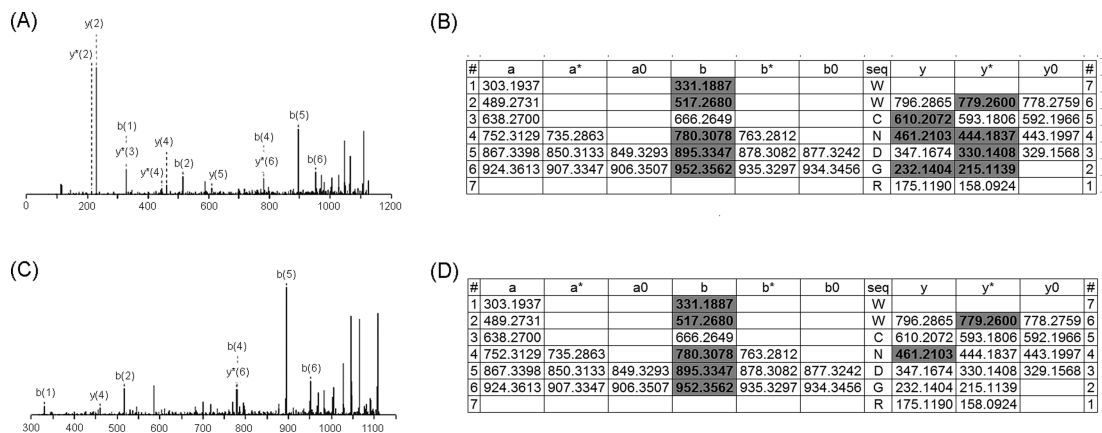


**Figure 3.** Comparison of WWCNDGR fragmentation in PQD and CAD modes. Peptide WWCNDGR from chicken lysozyme was labeled with iTRAQ reagent at the N-terminus. Adjacent spectra from PQD scan (A) and CAD scan (C) shows the fragmentation peak list of the same precursor in PQD and CAD modes, respectively. Fragment ions identified after database search in PQD and CAD scan were shown in (B) and (C), where shaded bold ions are those identified.

Iscove's Modified Dulbecco's Medium supplemented with 20% fetal bovine serum (Hyclone, Thermo Fisher Scientific, Inc., Waltham, MA), 100 U of penicillin, and 100  $\mu$ g of streptomycin per mL (Invitrogen, Carlsbad, CA). For protein extraction, SNU5 cells were lysed in 8 M urea and 20 mM HEPES supplemented with complete protease inhibitor cocktail tablets (Roche, Nutley, NJ). All chemicals were purchased from Sigma-Aldrich (St. Louise, MA) unless otherwise stated.

Proteins, either from standard protein mixture or SNU5 lysate, were tryptically digested and labeled with iTRAQ as previously described<sup>16</sup> with some modifications. Briefly, proteins were first reduced in 5 mM Tris-(2-carboxyethyl) phosphine (TCEP) for 1 h at 30  $^{\circ}$ C, followed by blocking cysteine residues in 10 mM methylmethanethiosulfate (MMTS) for 15 min at room temperature, before digestion with sequencing-grade modified trypsin (Promega, Madison, WI). Peptides were dried via vacuum, dissolved again in 0.5 M TEAB, and labeled with iTRAQ reagents (Applied Biosystems, Foster City, CA). The

labeling scheme for 7 standard proteins mixture (Table 2 in Supporting Information) was 114, 50  $\mu$ g; 115, 200  $\mu$ g; 116, 100  $\mu$ g; 117, 100  $\mu$ g, with a distribution profile of 1:4:2:2. For 6 standard proteins mixture (Table 3 in Supporting Information) was 114, 100  $\mu$ g; 115, 100  $\mu$ g; 116, 200  $\mu$ g; 117, 50  $\mu$ g, with a distribution profile of 1:1:2:0.5. For SNU5 lysate, 114 was 100  $\mu$ g; 115 was 100  $\mu$ g; 116 was 50  $\mu$ g; 117 was 200  $\mu$ g, with a distribution profile of 1:1:0.5:2. Peptides from the standard protein mixture were subsequently desalted using SEP-PAK C18 cartridges (Waters Corporation, Milford, MA) and dried using vacuum centrifugation. Dried peptides were stored in  $-80$   $^{\circ}$ C before MS analysis.

**Strong Cation Exchange Fractionation.** Labeled peptides from SNU5 cell lysate were fractionated using a PolySULFO-ETHYL A column (4.6 mm  $\times$  100 mm, 5  $\mu$ m particle size, 200  $\text{\AA}$  pore size) (PolyLC, Columbia, MD) on a Shimadzu Prominence UFLC system (Kyoto, Japan). A 50-min gradient was designed for SNU5 peptides separation using a combination

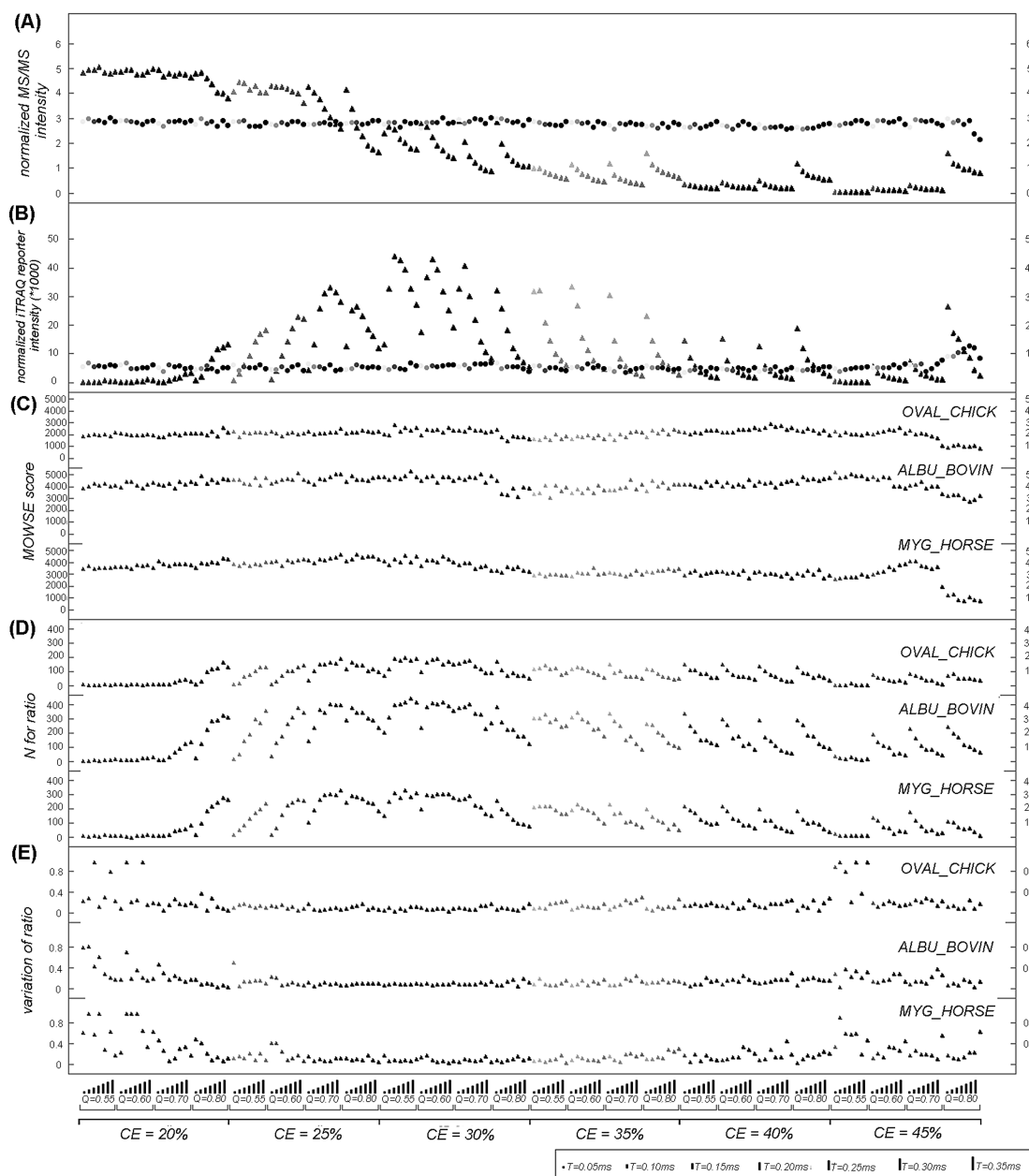


**Figure 4.** Comparison of 168 different PQD-CAD hybrid MS/MS scan configurations using 6 standard protein mixture (Table 3 in Supporting Information). Normalized MS/MS intensity (A), iTRAQ reporter intensity (B), MOWSE score (C), number of iTRAQ reporter qualified by Mascot (D), and variation of Ratio (E) of three selected proteins were compared. Circles: CAD (CE = 35%,  $Q = 0.25$ ,  $T = 30$  ms). Triangles: PQD.

of 10 mM  $\text{KH}_2\text{PO}_4$  in 25% acetonitrile, pH 2.85 (buffer A) and buffer A with 500 mM KCl, pH 2.85 (buffer B). The gradient consisted of isobaric buffer A for 5 min, followed by 0–10% buffer B over 2 min, 10–15% buffer B over 20 min, subsequently 15–40% buffer B over 8 min, after that 40–100% buffer B over 5 min, and finally 100% buffer B for 5 min. A total of 15 fractions were collected, followed by vacuum drying and desalting using SEP-PAK C18 cartridges. Dried peptides were stored at  $-80^\circ\text{C}$  before MS analysis.

**LC-MS/MS Analysis.** Peptide samples from standard protein mixtures or fractionated SNU5 cell lysates were dissolved in 0.1% formic acid, and analyzed using conditions described below. The LTQ Orbitrap, or LTQ FT Ultra (Thermo Fisher Scientific, Inc., Bremen, Germany) was coupled with an online

Shimadzu UFLC system utilizing nanospray ionization (Michrom Bioresources, Inc., Auburn, CA). Peptides were first enriched using a Zorbax 300SB C18 column (5 mm  $\times$  0.3 mm, Agilent Technologies, Santa Clara, CA) followed by elution into an integrated nanobore column (75  $\mu\text{m}$   $\times$  100 mm, New Objective, Woburn, MA) packed with C18 material (5  $\mu\text{m}$  particle size, 300  $\text{\AA}$  pore size, Michrom BioResources, Inc.). Mobile phase A (0.1% formic acid) and mobile phase B (0.1% formic acid, 100% acetonitrile) were used to establish the acetonitrile gradient. A 45-min gradient was used to fractionate the standard protein mixture, and comprised 8–35% buffer B linear gradient over 26 min, 35–60% buffer B over 6 min, followed by 60–80% buffer B for 1 min, maintaining at 80% buffer B for 2 min, and finally decreasing to 8% buffer B, which was maintained for 10



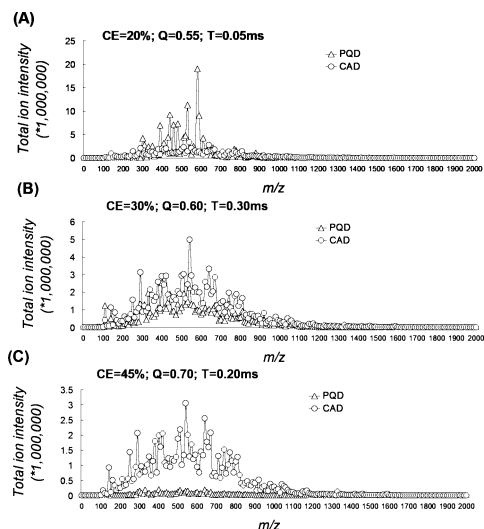


**Figure 5.** Comparison of MS/MS fragment ion  $m/z$  distribution of 3 typical PQD–CAD hybrid settings. CAD setting was CE = 35%,  $Q = 0.25$ ,  $T = 30$  ms. PQD was set to (A) CE = 20%;  $Q = 0.55$ ;  $T = 0.05$  ms; (B) CE = 30%,  $Q = 0.60$ ,  $T = 0.30$  ms; (C) CE = 45%,  $Q = 0.70$ ,  $T = 0.20$  ms.

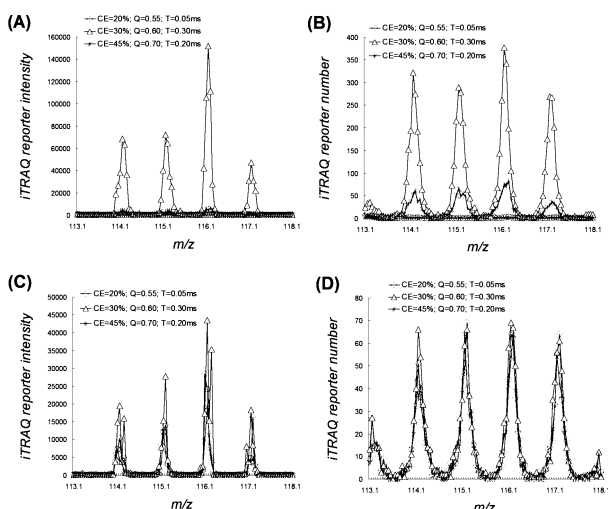


**Figure 6.** Comparison of iTRAQ reporter detection of 3 typical PQD–CAD hybrid settings. CAD setting was CE = 35%,  $Q = 0.25$ ,  $T = 30$  ms. PQD was set to (1) CE = 20%;  $Q = 0.55$ ;  $T = 0.05$  ms; (2) CE = 30%,  $Q = 0.60$ ,  $T = 0.30$  ms; (3) CE = 45%,  $Q = 0.70$ ,  $T = 0.20$  ms. Total iTRAQ reporter intensity and number from PQD (A and B) and CAD (C and D) were depicted.

min. Peptides from SNU5 cell lysate samples were subjected to a 90-min gradient, consisting of 5% buffer B for the first 3 min, followed by a linear gradient from 5% to 8% buffer B over 3 min, then 8–27.5% buffer B over 52 min, 27.5–60% buffer B over 18 min, 60–80% buffer B over 1 min, and finally 80% buffer B for 5 min before reduction to 5% buffer B for the last 8 min.

The MS analysis was done in either LTQ Orbitrap or LTQ FT Ultra as described previously<sup>17</sup> with some modifications. Briefly, the LTQ was operated in a data-dependent mode by performing MS/MS scans for the maximum 5–10 most intense peaks (ion selection threshold of 500 counts) from each MS scan. In PQD–CAD hybrid mode, each precursor ion was first analyzed in PQD mode, followed by CAD mode (Figure 1B). Samples were injected into the MS with an electrospray potential of 1.8 kV without sheath or auxiliary gas flow. Ion

transfer tube temperature was set to 180 °C and collision gas pressure at 0.85 mTorr. The MS scan range was 350–2000  $m/z$ . Dynamic exclusion was activated with a repeat count of 1, and exclusion duration of 30 s. Isolation width was set to 2, and default charge state was 5. For CAD mode, normalized collision energy (CE) was set to 35%, activation  $Q$  ( $Q$ ) was set to 0.25, and activation time ( $T$ ) at 30 ms. For PQD mode, a total of 168 different settings were systematically tested. CE varied from 20% to 45%,  $Q$  from 0.55 to 0.80, and  $T$  from 0.05 ms to 0.35 ms. Spectra were stored in centroid format in raw data files with XCalibur (version 2.0 SR2).

**Bioinformatics.** Raw data files generated from LTQ Orbitrap or LTQ FT Ultra were converted into XML file format using BioworksBrowser 3.3 (Thermo Fisher Scientific, Inc., Bremen, Germany). Peak lists were extracted from XML files and formatted as mascot generic files using an in-house perl script called “XML2mascot”. Raw data files were also converted into peak lists in the format of dta files using “extract\_msn.exe” (version 4.0) (Thermo Fisher Scientific, Inc., Bremen, Germany), followed by conversion into mascot generic file format using an in-house perl script called “dta2mascot”.<sup>17</sup> Mascot generic files were then submitted to Mascot server (version 2.2.03) for database search and quantitation. MS and MS/MS total ion intensity for PQD and CAD, as well as iTRAQ reporter total ion intensity were extracted from mascot generic files using in-house perl scripts. MS/MS total ion intensity was normalized against MS total ion intensity as shown in the following formula:

$$\text{Normalized Total Ion Intensity}_{\text{MS/MS}} = \frac{\text{Total Ion Intensity}_{\text{MS/MS}}}{\text{Total Ion Intensity}_{\text{MS}}} * 1000 \quad (1)$$

where  $\text{Total Ion Intensity}_{\text{MS/MS}}$ ,  $\text{Total Ion Intensity}_{\text{MS}}$ , and  $\text{Normalized Total Ion Intensity}_{\text{MS/MS}}$  represent MS/MS total ion intensity, MS total ion intensity, and normalized MS/MS total ion intensity, respectively.

Comparison of results generated from large number of iTRAQ experiments was done and presented graphically with in-house perl scripts. Overall variation of iTRAQ ratio was calculated according to the following formula:

$$\text{Variation Of Ratio} = \sqrt{\frac{(\text{Ratio}_{115/114} / \text{TRatio}_{115/114} - 1)^2 + (\text{Ratio}_{116/114} / \text{TRatio}_{116/114} - 1)^2 + (\text{Ratio}_{117/114} / \text{TRatio}_{117/114} - 1)^2}{2}} \quad (2)$$

where  $\text{Ratio}_{115/114}$ ,  $\text{Ratio}_{116/114}$ , and  $\text{Ratio}_{117/114}$  represent the reported 115/114 ratio, 116/114 ratio, and 117/114 ratio, respectively;  $\text{TRatio}_{115/114}$ ,  $\text{TRatio}_{116/114}$ , and  $\text{TRatio}_{117/114}$  represent the theoretical ratio for 115/114, 116/114, and 117/114, respectively;  $\text{Variation Of Ratio}$  represents the overall variation of iTRAQ ratio.

Peptide/protein identification and quantitation information generated by Mascot server in the format of csv files were converted into tab-separated files using an in-house perl program. Protein identification and iTRAQ quantitation were done by searching the combined data against in-house standard protein databases or International Protein Index (IPI) human protein database (version 3.34; 67 758 sequences) supplemented with trypsin via Mascot server (version 2.2.03). In order to estimate the rate of false positives (FP), the search was performed with “target” (forward IPI human sequence) and “decoy” (reverse IPI human sequence) databases as described elsewhere.<sup>18</sup> Minimum MOWSE score for protein identification and quantitation was adjusted accordingly to ensure the FP < 1%. The search was limited to maximum 2 missed trypsin

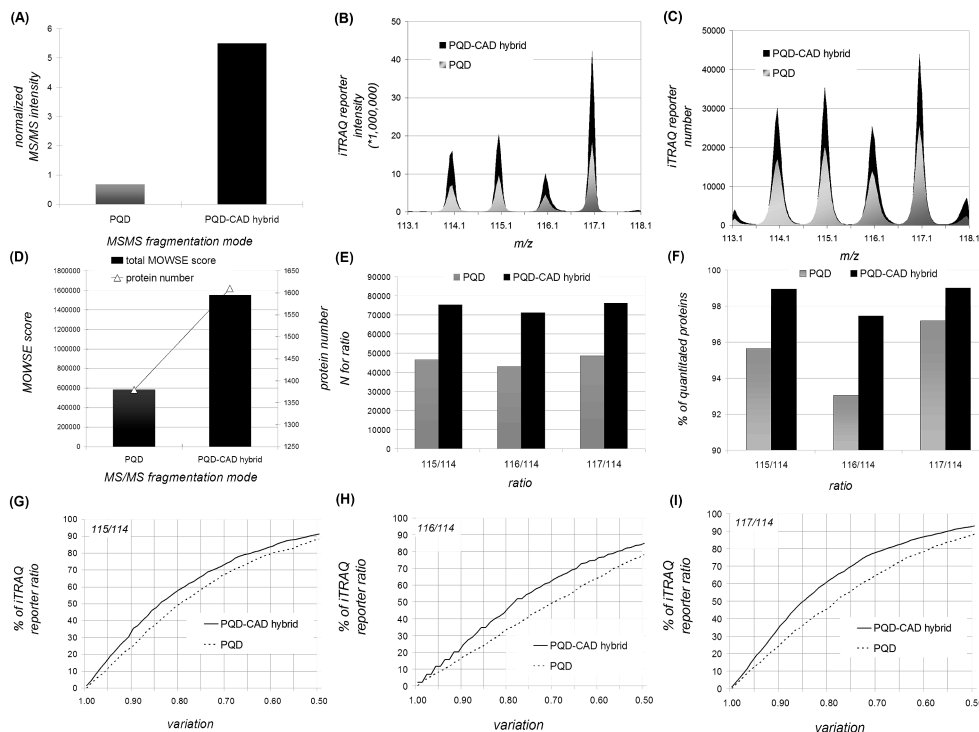


**Figure 7.** Comparison of PQR and PQR–CAD hybrid for iTRAQ quantitation with SNU5 cell lysate. PQR was done in a default setting (CE = 35%;  $Q = 0.70$ ;  $T = 0.10$  ms); PQR–CAD hybrid employed an optimized setting (PQR: CE = 30%;  $Q = 0.60$ ;  $T = 0.30$  ms. CAD: CE = 25%,  $Q = 0.25$ ,  $T = 30$  ms). Normalized MS/MS intensity (A), total iTRAQ reporter intensity (B), iTRAQ reporter number detected (C), sum of protein number and MOWSE score (D), number of iTRAQ reporter qualified by Mascot (E), percentage of quantitated proteins by Mascot (F), and accuracy of iTRAQ quantitation (G–I) were shown.

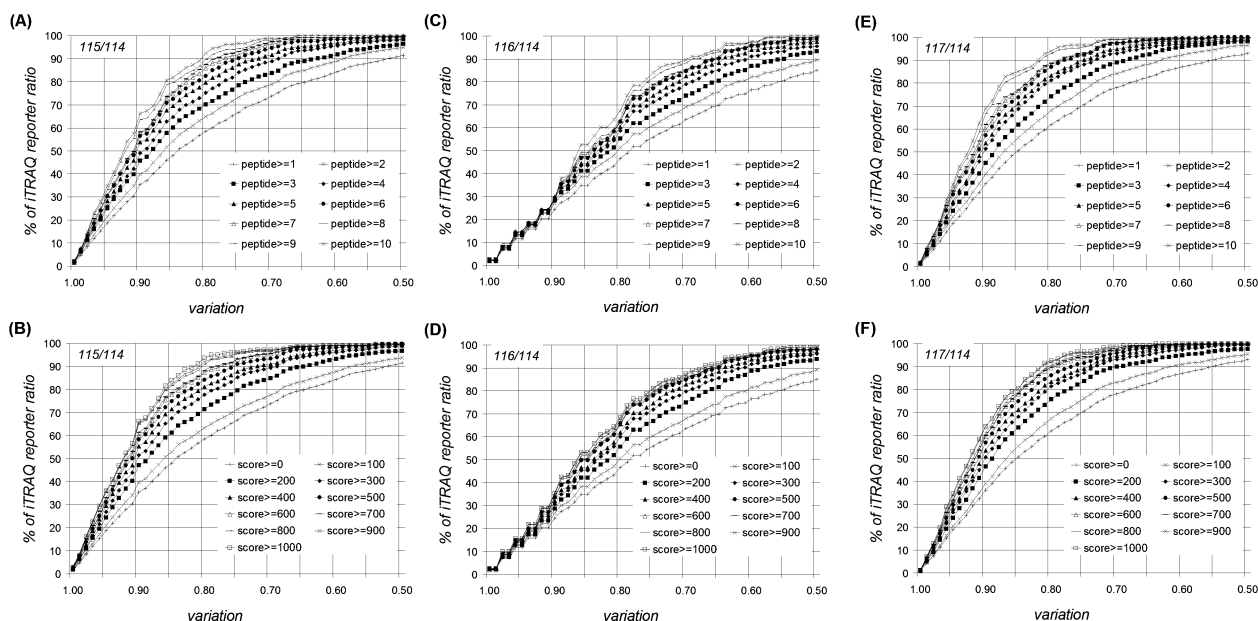


**Figure 8.** iTRAQ quantitation of SNU5 with PQR–CAD hybrid mode. Accuracy of iTRAQ quantitation is correlated to amount of protein (117 > 114, 115 > 116, ratio of amount of proteome used 2(117):1(114):1(115):0.5(116)) in the sample, number of unique peptides identified per protein (A, C, E) and Mascot score (B, D, F).

cleavages; no.  $^{13}\text{C}$  of 2; mass tolerances of 20 ppm for peptide precursors; and 0.8 Da mass tolerance for fragment ions. MMTS of cysteine, iTRAQ reagent labeling at N-terminal and lysine were set as fixed modifications. Variable modifications included oxidation of methionine, iTRAQ reagent labeling at tyrosine, phosphorylation of serine, threonine, and tyrosine. The resulting data sets were further analyzed using in-house perl scripts accordingly (Figure 1A).

## Results and Discussion

**CAD and PQR Both Play Indispensable Roles in iTRAQ-based Quantitation.** PQR was introduced as a novel fragmentation method to eliminate the low mass cutoff in linear ion trap MS. It has been shown to take identical time as CAD but with a slightly weaker fragmentation capacity.<sup>11,13</sup> To make full use of these two fragmentation methods, it is crucial to



understand the benefits and drawbacks of the two. Here we first tested a 7-protein mixture sample via PQD and CAD modes in linear ion trap MS, respectively. The default CAD setting here was  $CE = 35\%$ ,  $Q = 0.25$ ,  $T = 30$  ms; while the default PQD setting was  $CE = 30\%$ ,  $Q = 0.70$ ,  $T = 0.10$  ms. Experiments were performed twice to test reproducibility. In these experiments, total ion chromatograms at MS level were identical (data not shown) in both modes, whereas MS/MS total ion intensity in CAD mode was approximately 2.5-fold as high as that in PQD mode (Figure 2A), indicating that generally PQD is a less efficient fragmentation method.

PQD, through subtle manipulation of  $Q$ -value,<sup>11</sup> maintains the equilibrium in a single MS/MS fragmentation process between enough energy endowment to precursor ions that drive fragmentation, and proper electromagnetic field intensity for stability of low  $m/z$  fragment ions. However, PQD merely activates precursors for shorter than 0.5 ms, whereas activation time in CAD is as long as 30 ms. The remarkable difference of activation time provides clues as why ions are generally more vulnerable to be fragmented in CAD than those in PQD.

However, PQD is not always a less efficient fragmentation method than CAD. We found that PQD produced better signals than CAD in certain cases. PQD shows more abundant low  $m/z$  ions as a consequence of eliminating the "one-third rule".<sup>11,13</sup> As shown in Figure 3, a small peptide WWCNDGR ( $m/z = 936.0187$ ) from chicken lysozyme, which was labeled at the N-terminus with 4-plex iTRAQ reagent, was subsequently fragmented in both PQD and CAD mode. PQD generated 12 of 38 theoretical fragment ions, while CAD only produced 7. PQD detected 5 more  $y$  ions than CAD; furthermore, PQD provided iTRAQ signals. This example illustrates that PQD is superior to CAD in the case of fragmenting low mass precursors.

On the other hand, CAD is not always an inferior fragmentation method for iTRAQ quantitation in linear ion trap MS. We investigated the  $m/z$  distribution of precursors which produced detectable iTRAQ reporter ions in both PQD and CAD. Results illustrated that CAD detected stronger iTRAQ reporter ion signals than PQD if precursor ions were lower than 500  $m/z$ . On the other hand, CAD cannot detect iTRAQ reporter ions precursor  $m/z$  above 500. In contrast, PQD detected iTRAQ signals from precursors of the entire  $m/z$  range (Figure 2B). The results suggested that CAD is a robust fragmentation method for iTRAQ quantitation when precursors are lower than 500  $m/z$ .

Next, we inspected the iTRAQ reporter capturing efficiency of PQD and CAD. After summation of all reporter ions' intensities, the two modes agreed with each other by showing four sharp peaks, at  $m/z$  114.1, 115.1, 116.1, and 117.1, expressing approximately the 1:4:2:2 distribution profiles as shown in Figure 2C. This verifies that CAD, like PQD, also accurately detects the iTRAQ signals. Interestingly, the iTRAQ reporter total ion intensity in CAD was over 4-fold higher than that in PQD, signifying that CAD is not inferior to PQD in generating and detecting iTRAQ reporter ions. Nevertheless, the iTRAQ reporter number detected in PQD mode was over 2-fold more than that in CAD (Figure 2D), suggesting that fewer iTRAQ reporter ions were detected in CAD. This is in line with the previous observation that PQD detected iTRAQ from full range  $m/z$  precursors; whereas CAD only detected those from low  $m/z$  precursors (Figure 2B).

Taken together, CAD generally produces stronger signals from fragment ions and iTRAQ reporter ions than PQD. Specifically when the precursor  $m/z$  is low, CAD is a poorer

fragmentation method but still generates higher iTRAQ reporter intensity. In view of the diverse precursor  $m/z$  values in a complex biological sample, this result supports that PQD and CAD both play indispensable roles in identification and iTRAQ quantitation in linear ion trap MS. Integration of these two modes might be a preferable way to achieve better performance for iTRAQ quantitation in linear ion trap MS.

**Hybridization of PQD and CAD.** We developed a PQD–CAD hybrid fragmentation mode for iTRAQ quantitation of complex biological samples in linear ion trap MS which integrates the complementary advantages of CAD and PQD. On the basis of LTQ Orbitrap and LTQ FT Ultra, we designed an MS/MS scan mode which is composed of a PQD scan and a subsequent CAD scan for each precursor ion. Five to 10 PQD–CAD hybrid pairs were coupled with each MS scan (Figure 1B). The MS instrument settings for PQD–CAD hybrid fragmentation mode is quite straightforward since users do not need to equip external device or software to their LTQ instruments.

Comparatively, bioinformatics processing of the resulting data files is more challenging. PQD–CAD hybrid mode generates raw data files where each MS spectrum is followed by pairs of PQD–CAD spectra and each PQD–CAD spectrum pair originated from the same precursor. We first converted raw data files into extensible markup language (XML) format, a widely accepted data interchange standard in proteomic applications<sup>19</sup> using BioworksBrowser (version 3.3). Consequently, peak lists were extracted and converted to mascot generic files from the XML files using a perl script called "XML2mascot". Peak lists were also generated by extract\_msn.exe (version 4.0) in dta file format. We developed a perl program called "dta2mascot" to generate mascot generic files. To integrate the adjacent PQD and CAD spectra for the same precursor, two alternative approaches have been employed. (1) Grouping method: dta files were generated using extract\_msn.exe with the grouping switch on. This approach automatically combines the adjacent PQD and CAD spectra into one dta file. (2) Reporter migrating method: extract\_msn.exe was executed with switch G0 and S0 on to generate all dta spectra. The adjacent PQD and CAD spectra are processed separately into two dta files. To retain quantitative information, we developed a program called "PQD–CAD hybridizer" to integrate quantitative information, where iTRAQ reporter ions from PQD spectra were copied to CAD spectra. The grouping method reduced the total number of dta spectra to half and speeded up the database search. However, the grouping of spectra introduced noise and resulted in poor protein identification score (data not shown). The reporter migrating method is the preferred method. CAD generated strong fragmentation for good protein identification; the missing iTRAQ reporter in CAD spectrum was borrowed from the PQD spectrum.

**Optimization of PQD–CAD Hybrid.** In PQD mode, three parameters determine the PQD efficiency.<sup>8,13</sup> (a) Normalized collision energy (CE) is the value for normalized collision energy employed in resonance excitation process. The value, indicated using a scale of 0–100%, determines the fragmentation efficiency of precursor ions. (b) Activation  $Q$  ( $Q$ ) value represents the elevated  $Q$ -value to allow precursor ions to gain enough kinetic energy before fragmentation. In CAD mode,  $Q$  is usually set to 0.25, while in PQD mode,  $Q$  is normally higher than 0.55. (c) Activation time ( $T$ ) stands for the duration time to allow the precursors to fragment. In PQD, this parameter normally ranges from 0.05 to 0.35 ms, while it is typically 30 ms in CAD mode.<sup>8,15</sup>

To find the best configuration for PQD–CAD hybrid mode, we fixed the default CAD setting ( $CE = 35\%$ ,  $Q = 0.25$ ,  $T = 30$  ms) and adjusted three PQD parameters ( $CE$ ,  $Q$ , and  $T$ ) in a stepwise manner by analyzing a total of 168 iTRAQ-labeled standard protein samples in an uninterrupted manner. For  $CE$ , we tested 6 conditions: 20%, 25%, 30%, 35%, 40%, and 45%; for  $Q$ , four values were tested including 0.55, 0.6, 0.7, and 0.8; for  $T$ , 7 durations (0.05, 0.10, 0.15, 0.20, 0.25, 0.30, and 0.35 ms) were tested (Table 1 in Supporting Information). In each condition, 5 PQD–CAD hybrid pairs were coupled with each MS scan (Figure 1B). The same experiment was replicated on another date after MS instrument recalibration, as shown in Figure 1 in Supporting Information. Results from these two independent experiments demonstrated the reproducibility of the workflow, although the iTRAQ reporter intensity was sensitive to other instrument settings and calibration as revealed by Figure 4B and Figure 1B in Supporting Information.

We first examined total ion intensity for each condition (Figure 4A). The circles show that total ion intensities in CAD mode across the 168 conditions are fairly constant, agreeing with our experiment design where we have fixed the CAD parameters; it also serves as evidence for the reliable reproducibility of 168 individual experiments. The triangles show total ion intensity in PQD mode. Interestingly, these triangles vary in the shape of smooth curves grouped by increasing  $T$  when  $CE$  and  $Q$  are fixed. Generally, total ion intensity in PQD mode decreases when  $T$  is increased. The total ion intensity in PQD mode was higher than its counterpart case in CAD mode when  $CE$  was set to a low value (20%, 25%) (Figures 4A and 5A). MS/MS spectra inspection suggested that most precursors in these low  $CE$  conditions were not properly fragmented, and as a result, total ion intensities were kept innately high (data not shown). As shown in Figure 5A, MS/MS spectra of a typical low  $CE$  PQD ( $CE = 20\%$ ,  $Q = 0.55$ ,  $T = 0.05$  ms) revealed that there were very few ions below 300  $m/z$ . It further supports the view that precursors are not well fragmented in these low  $CE$  conditions. Alternation of  $Q$  and  $T$  did not improve the PQD efficiency much, indicating  $CE$  is a dominant factor for PQD efficiency. When  $CE$  increased to 35% or higher, precursors fragmented well (data not shown). Total ion intensity in PQD mode decreased to a level lower than that in CAD mode (Figures 4A and 5C). The reason may be that overloaded energy fragments precursor ions thoroughly into small ions that cannot be trapped in linear ion trap MS. It signifies that high energy imparted to the precursors tempers ion capturing capability in ion trap MS. The low  $CE$  and high  $CE$  groups shared similar identification efficiency (Figure 4C), suggesting that fragment ions generated by PQD mode contributed very little to protein identification compared with those by CAD mode.

We next examined iTRAQ reporter total ion intensity in these conditions (Figure 4B). The circles representing CAD mode shapes as a horizontal line which could also be taken as an internal control for the 168 PQD–CAD hybrid conditions. The base level of iTRAQ reporter total ion intensity in CAD mode re-enforces the notion that CAD also detects iTRAQ reporter ions. The triangles representing PQD shows that total intensity of iTRAQ reporter ions is highly depended on instrumental settings. Low  $CE$  and high  $CE$  conditions generated very few iTRAQ reporter ions, which were even fewer than those in CAD mode. Generally, in low  $CE$  conditions (20%, 25%), iTRAQ reporter total ion intensity increased when  $T$  or  $Q$  were amplified, indicating the precursors were not properly fragmented in those conditions, and more energy was compulsory

for proper fragmentation. On the other hand, precursors fragmented better in high  $CE$  conditions (data not shown). iTRAQ reporter total ion intensity declined sharply when  $T$  was increased, but was not significantly influenced when  $Q$  was changed, suggesting overloaded energy to the precursor ions did decrease, instead of improve, iTRAQ reporter ion capturing capability. iTRAQ reporter total ion intensity reached maximum when  $CE$  was set to a medium level. Most favorable  $Q$  and  $T$  values in these conditions varied according to different  $CE$ . These conditions vary slightly in the replicate study (Figure 1 in Supporting information), suggesting the optimized condition is also dependent on the other instrumental settings and calibration.

We selected three typical conditions with different  $CE$ , and extracted from PQD spectra ions with an  $m/z$  ranging from 113.1 to 118.1 (Figure 6A). These ions demonstrate in the shape of four peaks around 114.1, 115.1, 116.1, and 117.1 in PQD condition ( $CE = 30\%$ ,  $Q = 0.60$ ,  $T = 0.30$  ms). Peak area ratio correlated with the correct ratio 1:1:2:0.5, whereas the other two conditions form relatively weak peaks compared with this condition. iTRAQ reporter ions from CAD spectra were also demonstrated as four sharp peaks with approximately the correct ratio. No significant difference could be observed across the three conditions (Figure 6C). Analysis of iTRAQ reporter number also supports the conclusion (Figure 6B, D).

To validate the quantitative results of our bioinformatics analysis on the spectra, we extracted peak lists from raw data and converted them into mascot generic file format, followed by submitting to Mascot server (version 2.2.03) for protein database search and iTRAQ quantitation. MOWSE score<sup>20</sup> is a rational parameter to evaluate probability of protein presence in biological samples as well as the MS instrumental conditions for protein analysis. We used the MOWSE score of individual protein identified in our experiment to objectively evaluate different MS settings for iTRAQ protein quantitation and identification. As shown in Figure 4C, MOWSE scores of three typical proteins form a horizontal line, suggesting identification capability was not affected much when PQD parameters were adjusted. It reconfirms the conclusion that PQD contributes little to identification in PQD–CAD hybrid mode. The number of peptides contributed to iTRAQ ratio calculation ( $N$  for ratio) represents the quality of iTRAQ reporter detection in MS/MS spectra. As shown in Figure 4D, the pattern of distribution is quite similar to Figure 4B. Finally, differences between calculated ratios and the preset values, that is, variation of ratio, was compared. Medium  $CE$  groups showed best accordance (Figure 4E). These data further support that PQD parameters determine iTRAQ quantitation efficiency and optimal conditions are composed of medium  $CE$ .

The global stepwise comparison demonstrates PQD parameters contribute little to identification, but determine iTRAQ quantitation in the PQD–CAD mode. Favorable conditions are those with medium  $CE$ . Specifically, iTRAQ quantitation efficiency reaches peak when  $CE$  was around 30%. Optimal  $Q$  and  $T$  vary depending on  $CE$  value.

**Validation of PQD-CAD Hybrid Mode in Complex Biological Samples.** To test the applicability of the optimized PQD–CAD hybrid setting and the related bioinformatics algorithm for iTRAQ quantitation of complex biological samples, we employed the workflow to profile the proteome of a gastric cancer cell line, SNU5. At present, no study has yet addressed the proteome of SNU5. iTRAQ reagents 114–117 were used to label four aliquots of SNU5 digest with the ratio of 1:1:0.5:2.

The labeled sample was subjected to SCX fractionation into 15 fractions, and LC-MS/MS analysis in LTQ Orbitrap in PQD-CAD hybrid mode (PQD: CE = 30%,  $Q = 0.60$ ,  $T = 0.30$  ms. CAD: CE = 35%,  $Q = 0.25$ ,  $T = 30$  ms). We also included another experiment using the default PQD setting (CE = 35%,  $Q = 0.70$ ,  $T = 0.10$  ms) for comparison. Results showed that the hybrid generated 710% higher total ion intensity (Figure 7A), 92% higher iTRAQ reporter intensity (Figure 7B), and 51% increase in iTRAQ reporter number over the default PQD settings (Figure 7C).

Next, we performed database search and iTRAQ quantitation of the two data sets using the Mascot server. FP for protein identification was controlled below 1% by adjusting the minimum MOWSE score for protein to 55. In total, the PQD-CAD hybrid method identified 1610 SNU5 proteins of diverse molecular functions based on Panther classification<sup>21</sup> as shown in Figure 2 in Supporting Information. The accuracy of the ratios for 115/114, 116/114 and 117/114 was calculated against different variations. The results were also subjected to filtering of peptide number and MOWSE score (Figure 8). For 115/114, ratios of more than 50% quantitated proteins were between  $1 \times 0.8 = 0.8$  and  $1/0.8 = 1.25$  (variation of 0.8). Around 90% quantitated proteins had correct ratios within the variation of 0.5. Better quantitation was attained for proteins with higher number of peptides identified or higher MOWSE scores (Figure 8A,B). Analysis of 116/114 and 117/114 were in line with 115/114 (Figure 8C–F).

Compared with the default PQD setting, the hybrid method identified 17% more proteins than those in PQD setting (Figure 7D). Summation of MOWSE scores of identified proteins was 165% higher (Figure 7D). Besides, Mascot qualified 61% more quantitated peptides for ratio calculations (Figure 7E) and 3.2% higher percentage of quantitated proteins in hybrid setting on average (Figure 7F). Moreover, the hybrid method generated more accurate ratios (Figure 7G–I).

Interestingly, we notice the accuracy of iTRAQ quantitation seems to be correlated to the amount of protein in the sample. The protein amount we labeled with 116 is a half of that with 115, and a quarter of that with 117. Results from standard PQD showed percentage of quantitated proteins for 116/114 ratio was the worst of the three; it was 2.6% less than that for 115/114, and 4.1% less than that for 117/114 (Figure 7F). In the PQD-CAD hybrid mode, the percentage of quantitated proteins for 116/114 was improved by 4.4% (Figure 7F), suggesting the hybrid mode is especially useful for quantitation of low abundance proteins in the sample.

**Abbreviations:** PQD, pulsed-Q dissociation; CAD, collision-activated dissociation; iTRAQ, isobaric tags for relative and absolute quantitation; SILAC, stable isotope labeling by amino acids in cell culture; CE, normalized collision energy; XML, extensible markup language; SCX, strong cation exchange; perl, practical extraction and report language; FP, false positives.

**Acknowledgment.** We thank Sai Kiang Lim and Paul Hon-sen Tan for invaluable suggestions and editorial help; Bin Cao, Randong Yuan, Chen Zhao, Wei Meng, Xin Li, Chhiti Pandey, Arnab Datta for stimulating discussions; and Xu Chao for computer programming help. Tiannan Guo was supported by a grant from the National Cancer Centre Singapore Research Foundation. This work is supported by grants from Ministry of Education (AcRF: T206B3211) and Biomedical Research Council (BMRC: 07/1/22/19/531) of Singapore.

**Supporting Information Available:** Supplementary Figure 1, comparison of 168 different PQD-CAD hybrid MS/MS scan configurations; Supplementary Figure 2, Panther classification of molecular function of SNU5 proteome identified with a customized PQD-CAD hybrid mode in linear ion trap MS; Supplementary Table 1, list of 168 PQD conditions used in optimization; Supplementary Table 2, list of 7 standard protein mixture employed in this study; Supplementary Table 3, list of 6 standard protein mixture employed in this study. This material is available free of charge via the Internet at <http://pubs.acs.org>.

## References

- (1) Ong, S. E.; Mann, M. Mass spectrometry-based proteomics turns quantitative. *Nat. Chem. Biol.* **2005**, *1* (5), 252–62.
- (2) Goshe, M. B.; Smith, R. D. Stable isotope-coded proteomic mass spectrometry. *Curr. Opin. Biotechnol.* **2003**, *14* (1), 101–9.
- (3) Tao, W. A.; Aebersold, R. Advances in quantitative proteomics via stable isotope tagging and mass spectrometry. *Curr. Opin. Biotechnol.* **2003**, *14* (1), 110–8.
- (4) Cox, J.; Mann, M. Is proteomics the new genomics. *Cell* **2007**, *130* (3), 395–8.
- (5) Ong, S. E.; Blagoev, B.; Kratchmarova, I.; Kristensen, D. B.; Steen, H.; Pandey, A.; Mann, M. Stable isotope labeling by amino acids in cell culture, SILAC, as a simple and accurate approach to expression proteomics. *Mol. Cell. Proteomics* **2002**, *1* (5), 376–86.
- (6) Ross, P. L.; Huang, Y. N.; Marchese, J. N.; Williamson, B.; Parker, K.; Hattar, S.; Khainovski, N.; Pillai, S.; Dey, S.; Daniels, S.; Purkayastha, S.; Juhasz, P.; Martin, S.; Bartlett-Jones, M.; He, F.; Jacobson, A.; Pappin, D. J. Multiplexed protein quantitation in *Saccharomyces cerevisiae* using amine-reactive isobaric tagging reagents. *Mol. Cell. Proteomics* **2004**, *3* (12), 1154–69.
- (7) Mayya, V.; Rezaul, K.; Cong, Y. S.; Han, D. Systematic comparison of a two-dimensional ion trap and a three-dimensional ion trap mass spectrometer in proteomics. *Mol. Cell. Proteomics* **2005**, *4* (2), 214–23.
- (8) Griffin, T. J.; Xie, H.; Bandhakavi, S.; Popko, J.; Mohan, A.; Carlis, J. V.; Higgins, L. iTRAQ reagent-based quantitative proteomic analysis on a linear ion trap mass spectrometer. *J. Proteome Res.* **2007**, *6* (11), 4200–9.
- (9) Want, E. J.; Cravatt, B. F.; Siuzdak, G. The expanding role of mass spectrometry in metabolite profiling and characterization. *Chem-BioChem* **2005**, *6* (11), 1941–51.
- (10) Schwartz, J. C.; Syka, J. P.; Quarmby, S. T. Improving the Fundamentals of MSn on 2D Ion Traps: New Ion Activation and Isolation Techniques. *53rd ASMS Conference on Mass Spectrometry*, San Antonio, TX, 2005.
- (11) Kiyonami, R.; Schlabach, T.; Schwartz, J.; Miller, K.; Taylor, L. Analysis of Low Mass Ions in Peptide Fragmentation Spectra With a Linear Ion Trap. *55th ASMS Conference on Mass Spectrometry*, Indianapolis, IN, 2007.
- (12) Prieto Conaway, M. C.; Peterman, S. M.; Zhang, J.; Schwartz, J. C. Glycopeptide Analysis with the Finnigan LTQ with vMALDI Source and Pulsed Q Collision Induced Dissociation (PQD). *55th ASMS Conference on Mass Spectrometry*, Indianapolis, IN, 2007.
- (13) Huang, Y.; Zhang, T.; Kiyonami, T.; Waddell, K. Optimizing Parameters in a Linear Ion Trap with PQD Functionality for Simultaneous Protein Identification and Quantitation from Complex Mixtures Using iTRAQ. *55th ASMS Conference on Mass Spectrometry*, Indianapolis, IN, 2007.
- (14) Schlabach, T.; Zhang, T.; Miller, K.; Kiyonami, R. Protein Identification and Quantification using an Ion Trap with Enhanced Detection in the Low Mass Range. *55th ASMS Conference on Mass Spectrometry*, Indianapolis, IN, 2007.
- (15) Bantscheff, M.; Eberhard, D.; Abraham, Y.; Bastuck, S.; Boesche, M.; Hobson, S.; Mathieson, T.; Perrin, J.; Raida, M.; Rau, C.; Reader, V.; Sweetman, G.; Bauer, A.; Bouwmeester, T.; Hopf, C.; Kruse, U.; Neubauer, G.; Ramsden, N.; Rick, J.; Kuster, B.; Drewes, G. Quantitative chemical proteomics reveals mechanisms of action of clinical ABL kinase inhibitors. *Nat. Biotechnol.* **2007**, *25* (9), 1035–44.
- (16) Gan, C. S.; Chong, P. K.; Pham, T. K.; Wright, P. C. Technical, experimental, and biological variations in isobaric tags for relative and absolute quantitation (iTRAQ). *J. Proteome Res.* **2007**, *6* (2), 821–7.
- (17) Sze, S. K.; de Kleijn, D. P.; Lai, R. C.; Khia Way Tan, E.; Zhao, H.; Yeo, K. S.; Low, T. Y.; Lian, Q.; Lee, C. N.; Mitchell, W.; El Oakley,

- R. M.; Lim, S. K. Elucidating the secretion proteome of human embryonic stem cell-derived mesenchymal stem cells. *Mol. Cell. Proteomics* **2007**, *6* (10), 1680–9.
- (18) Elias, J. E.; Gygi, S. P. Target-decoy search strategy for increased confidence in large-scale protein identifications by mass spectrometry. *Nat. Methods* **2007**, *4* (3), 207–14.
- (19) Orchard, S.; Apweiler, R.; Barkovich, R.; Field, D.; Garavelli, J. S.; Horn, D.; Jones, A.; Jones, P.; Julian, R.; McNally, R.; Nerothin, J.; Paton, N.; Pizarro, A.; Seymour, S.; Taylor, C.; Wiemann, S.; Hermjakob, H. Proteomics and Beyond: a report on the 3rd Annual Spring Workshop of the HUPO-PSI 21–23 April 2006, San Francisco, CA, USA. *Proteomics* **2006**, *6* (16), 4439–43.
- (20) Pappin, D. J.; Hojrup, P.; Bleasby, A. J. Rapid identification of proteins by peptide-mass fingerprinting. *Curr. Biol.* **1993**, *3* (6), 327–32.
- (21) Thomas, P. D.; Campbell, M. J.; Kejariwal, A.; Mi, H.; Karlak, B.; Daverman, R.; Diemer, K.; Muruganujan, A.; Narechania, A. PANTHER: a library of protein families and subfamilies indexed by function. *Genome Res.* **2003**, *13* (9), 2129–41.

PR800403Z